Eur J Nucl Med Mol Imaging (2013) 40:1077–1083
DOI 10.1007/s00259-013-2393-z

ORIGINAL ARTICLE

Discrepant uptake of the radiolabeled norepinephrine analogues hydroxyephedrine (HED) and metaiodobenzylguanidine (MIBG) in rat hearts

Christoph Rischpler · Kenji Fukushima · Takuro Isoda · Mehrbod S. Javadi · Robert F. Dannals · Roselle Abraham · Richard Wahl · Frank M. Bengel · Takahiro Higuchi

Received: 9 November 2012 / Accepted: 7 March 2013 / Published online: 29 March 2013

Abstract
Purpose ^{11}C-Hydroxyephedrine (HED) and radioiodinated metaiodobenzylguanidine (^{123}I/^{131}I-MIBG) are catecholamine analogue tracers for sympathetic nerve positron emission tomography/single photon emission computed tomography (PET/SPECT) imaging. In contrast to humans, rat hearts demonstrate high nonneural catecholamine uptake-2 in addition to neural uptake-1, the contributions of which to tracer accumulation are not fully elucidated.
Methods Wistar rats were studied using the following pretreatments: uptake-1 blockade with desipramine 2 mg/kg IV, both uptake-1 and -2 blockade with phenoxybenzamine 50 mg/kg IV, or control with saline IV. HED or ^{123}I-MIBG was injected 10 min after pretreatment, and rats were sacrificed 10 min later. Heart to blood tissue count ratio (H/B ratio) was obtained using a gamma counter. To determine regional tracer uptake, dual-tracer autoradiography was performed with HED and ^{131}I-MIBG in Wistar rats with chronic infarction by transient coronary occlusion and reperfusion and in healthy control rats. Local tracer distributions were analyzed, and the infarcted rats' local tracer distributions were compared with histology.
Results The H/B ratios in control hearts were 34.4±1.7 and 25.5±2.1 for HED and ^{123}I-MIBG, respectively. Desipramine led to a significant decrease in HED (3.2±0.5, $p<0.0001$), while there was no change in ^{123}I-MIBG (25.5±6.4, p=n.s.). Phenoxybenzamine led to a significant decrease in both HED and ^{123}I-MIBG (3.5±0.02, 4.3±0.7, $p<0.0001$). Only HED showed a subepicardium-subendocardium gradient in healthy control hearts which is consistent with physiological innervation, while ^{131}I-MIBG was evenly distributed throughout the myocardium. ^{131}I-MIBG uptake defect closely matched the scar area determined by histology [3.8±2.3 % (^{131}I-MIBG defect) vs 4.0±2.4 % (scar)]. However, the scar area was clearly exceeded by the HED uptake defect (9.1±2.2 %, $p<0.001$).
Conclusion HED uptake showed high specificity to neural uptake-1 in rat hearts. On the other hand, ^{123}I/^{131}I-MIBG demonstrated distinct characters of regional tracer distribution and uptake mechanism that are compatible with significant contribution of nonneural uptake-2.

C. Rischpler · K. Fukushima · T. Isoda · M. S. Javadi · R. F. Dannals · R. Wahl · F. M. Bengel · T. Higuchi
Division of Nuclear Medicine, The Russell H. Morgan Department of Radiology, Johns Hopkins University, Baltimore, MD, USA

C. Rischpler
e-mail: rischpler@gmail.com

R. Abraham
Division of Cardiology, Department of Medicine, Johns Hopkins University, Baltimore, MD, USA

C. Rischpler
Nuklearmedizinische Klinik und Poliklinik, Klinikum rechts der Isar, Ismaninger Straße 22,
81675 Munich, Germany

F. M. Bengel
Department of Nuclear Medicine, Hannover Medical School, Hannover, Germany

T. Higuchi
CHFC/Department of Nuclear Medicine, Würzburg University, Würzburg, Germany

T. Higuchi (✉)
Nuklearmedizinische Klinik und Poliklinik,
Universitätsklinikum Würzburg, Oberdürrbacher Straße 6,
Gebäude A4 EO Nuklearmedizin,
97080 Würzburg, Germany
e-mail: thiguchi@me.com

Keywords ^{11}C-Hydroxyephedrine · ^{123}I/^{131}I-Metaiodobenzylguanidine · Rat hearts

Introduction

The function of the autonomic sympathetic nervous system is crucial and implies fast reactions to physiological changes due to exercise, for example, where hemodynamic parameters like heart rate and stroke volume need to be adjusted rapidly. The cardiac sympathetic nerve innervation and activity are affected in various conditions, especially in cardiac diseases including coronary artery disease [1]. Particularly, the importance of cardiac sympathetic nerve activation in the initiation and development process of left ventricular cardiac remodeling needs to be emphasized [2, 3].

Nuclear medicine has powerful tools to assess the distribution and activity of sympathetic innervation. The most commonly used norepinephrine analogue radiotracers are ^{11}C-hydroxyephedrine (HED) for positron emission tomography (PET) and ^{123}I-metaiodobenzylguanidine (MIBG) for single photon emission computed tomography (SPECT). For the assessment of sympathetic nerves, these radiotracers need to be taken up by the neuronal-specific uptake-1 into sympathetic nerve terminals, leaving only a negligible amount to be taken up by the uptake-2 mechanism into nonneural cells. In human hearts, HED and MIBG have been established for this purpose in a number of clinical studies [2, 4–6].

The rat heart is a well-established model for various cardiac diseases including ischemic heart disease and had been widely used to investigate therapy approaches [7–9]. The recent introduction of dedicated high-resolution small animal SPECT and PET systems allows noninvasive assessment of radionuclide tracer distribution in rat hearts [10, 11]. This imaging assay is considered to be of significant value because it enables longitudinal experiments with multiple observations over time. However, since species differences are reported between hearts of rodents and large mammals including humans, the specificity of the tracer kinetics must be analyzed before applying those clinically established tracers in rodent models [12].

As a consequence, we aimed to determine the contributions of neural uptake-1 and nonneural uptake-2 to the accumulation of HED and ^{123}I/^{131}I-MIBG in the rat heart after pharmacological blockade of uptake-1 or uptake-1 and -2 as well as after induction of myocardial infarction.

Materials and methods

Radiopharmaceuticals

^{123}I-MIBG (AdreView™) and ^{131}I-MIBG were both kindly provided by GE Healthcare. ^{123}I-MIBG was used within 2 h after calibration time [specific activity 2 mCi/ml (74 MBq/ml), radiochemical purity >95 %].

HED was synthesized as previously described [13]. Analyses at the end of syntheses revealed specific radioactivities in the range of 370–740 GBq/μmol and radiochemical purities greater than 98 %.

Animals

For our experiments 32 male Wistar rats (Charles River Laboratories Inc., Wilmington, MA, USA) each weighing between 250 and 300 g were used. Animal protocols were approved by the Johns Hopkins Institutional Animal Care and Use Committee and conducted according to the Guide for the Care and Use of Laboratory Animals [14].

Ex vivo tissue counting study

Twenty-two healthy Wistar rats were maintained under anesthesia throughout the procedure with 2 % isoflurane. Rats were assigned to one of the following pretreatments which were administered via tail vein injection: (1) blockade of the uptake-1 with desipramine 2 mg/kg IV (Sigma-Aldrich Co., St. Louis, MO, USA), (2) blockade of both uptake-1 and -2 with phenoxybenzamine 50 mg/kg IV (Sigma-Aldrich Co., St. Louis, MO, USA), or (3) saline IV for establishment of a control group. Ten minutes after pretreatment application, the respective radiotracer HED (55.5 MBq) or ^{123}I-MIBG (0.5 MBq) was injected intravenously. Hearts and blood were harvested 10 min after tracer injection to obtain tissue counts using a gamma counter (2480 WIZARD^2 Automatic Gamma Counter, PerkinElmer, Waltham, MA, USA). Following weight and decay correction of tissue counts, the heart to blood tissue count ratio (H/B ratio) was calculated.

Dual-tracer autoradiography study

Myocardial infarction was performed in six healthy Wistar rats as previously described [7, 15]. Before initiation of the operation, anesthesia was induced and maintained throughout the whole procedure using isoflurane at a concentration of 1–3 % while ventilating animals artificially. Briefly, a left anterolateral approach was performed in order to visualize the heart and to locate the left anterior descending artery (LAD). Then the LAD was occluded for 20 min using a 7-0 polypropylene suture that was first pulled through the myocardial tissue beneath the LAD and then threaded through a small vinyl tube building a small snare. Subsequently reperfusion was accomplished by releasing the suture. Effective coronary occlusion and reperfusion were verified visually by identification of cyanosis or blush downstream from the suture following the respective procedure. To establish a group of sham-operated rats, four additional animals received the same

procedures exclusive of the execution of occlusion and reperfusion. Subsequently, animals' chests were closed, and the rats were allowed to recover and received appropriate postoperative pain medication.

After housing for 2 more months, rats were anesthetized again using 2 % isoflurane, and both HED (111 MBq) and ^{131}I-MIBG (0.0925 MBq) were injected via tail vein. After 10 min of tracer administration, hearts were harvested, frozen, and cut into 20-μm short axis slices using a cryostat (CM1800, Leica). Dual-tracer autoradiography was performed to assess HED and ^{131}I-MIBG uptake as described before [16]. To obtain the distribution of HED, autoradiography plates (Multi Sensitive Phosphor Screens, PerkinElmer, Waltham, MA, USA) were exposed to the short axis slices immediately for 45 min and thereafter imaged using a digital autoradiographic system (Cyclone Storage Phosphor scanner, Packard). Twelve hours later, after complete decay of ^{11}C, the tissue samples were again imaged for the distribution of ^{131}I-MIBG by exposing autoradiography plates for 3 weeks. Subsequently, for determination of the scar area, the short axis slices were stained using the standard Verhoeff-van Gieson (VVG) staining procedure.

All obtained images were then analyzed using the ImageJ software (National Institutes of Health; http://rsbweb.nih.gov/ij/) [17]. To quantify autoradiography tracer uptake distribution pattern in noninfarcted control hearts, regions of interest (ROIs) were drawn for the anterior, lateral, septal, and inferior walls on midventricular short axis slices. In addition, to measure transverse distribution pattern, ROIs were drawn in the subepicardial and in the subendocardial wall portion. Obtained results (dpm/mm^2) were then normalized to account for differences in the amount of tracer injected. In the infarcted hearts, scar area and area of tracer uptake defect were determined by manual contouring in midventricular short axis slices using digitally obtained photography images of VVG and autoradiographic images, respectively. Then, percentages of the scar and tracer uptake defect area in left ventricular short axis slices were calculated.

Statistical analysis

All results are displayed as mean ± SD. The two-tailed paired Student's t test was used to compare differences between two dependent groups, and the two-tailed independent Student's t test for differences between independent groups. Multiple group comparisons were performed using analysis of variance (ANOVA). Correlations are expressed as R^2 indicating the Pearson correlation coefficient. A p value of less than 0.05 was assumed to be statistically significant. MedCalc for Windows, version 11.6.1.0 (MedCalc Software, Mariakerke, Belgium) was used for all statistical analysis.

Results

Ex vivo tissue counting of HED and ^{123}I-MIBG in rats: controls, after blockade of uptake-1, and after blockade of uptake-1 and -2

Figure 1 summarizes the results of the ex vivo tissue counting study for HED and ^{123}I-MIBG. The H/B ratio of HED was 34.4±1.7 in the control group. There was a significant decrease of the H/B ratio to 3.2±0.5 ($p<0.0001$) after blocking the uptake-1 with desipramine 2 mg/kg. After blockade of both uptake-1 and -2 by the administration of phenoxybenzamine 50 mg/kg, there was no additional decline of the H/B ratio (3.5±0.02, $p<0.0001$ vs control, p = n.s. vs uptake-1 blockade). This indicates the high specificity of HED uptake for the uptake-1 mechanism.

For ^{123}I-MIBG the H/B ratio in the saline-treated control group was 25.5±2.1 and did not change after uptake-1 blockade (25.5±6.4, p = n.s.). However, pretreatment with

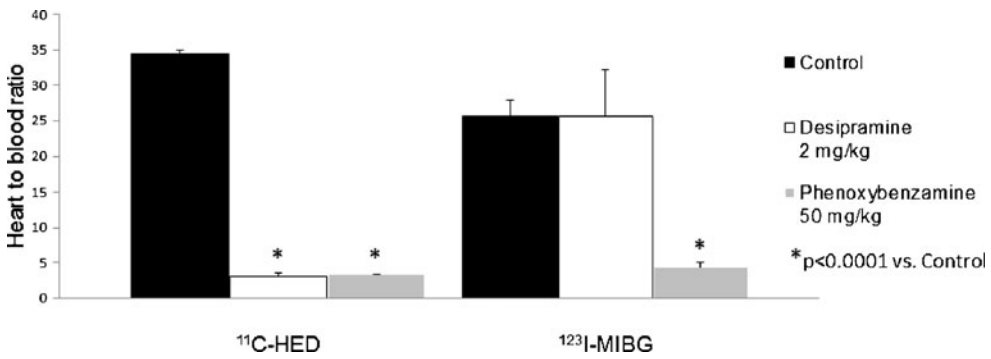

Fig. 1 Results of the ex vivo tissue counting study. Using ^{11}C-HED, the heart to blood tissue count ratio (H/B ratio) decreases significantly after blockade of uptake-1 with desipramine 2 mg/kg. There is no additional drop of the H/B ratio after administration of the uptake-1 and -2 blocker phenoxybenzamine 50 mg/kg indicating specificity of HED to uptake-1. Using ^{123}I-MIBG, however, the H/B ratio is not affected by the blockade of uptake-1 with desipramine 2 mg/kg. The H/B ratio declines significantly only after administration of the uptake-1 and -2 blocker phenoxybenzamine 50 mg/kg

the uptake-1 and -2 blocker phenoxybenzamine led to a significant drop of the H/B ratio to 4.3±0.7 ($p<0.0001$ vs control, $p<0.002$ vs uptake-1 blockade) suggesting significant contribution of tracer uptake via the nonneural uptake-2 mechanism.

Dual-tracer autoradiography of HED and ^{131}I-MIBG in the healthy myocardium and in a chronic model of coronary occlusion and reperfusion

Both HED and MIBG showed homogeneous distribution among the left ventricular walls within the healthy myocardium [anterior, septal, inferior, and lateral walls: 7,382±374, 6,958±446, 7,334±642, and 7,513±444 dpm/mm^2, n.s. (HED); 7,657±67, 7,626±233, 7,719±306, and 7,992±63 dpm/mm^2, n.s. (^{131}I-MIBG), respectively]. However, the accumulation of ^{11}C-HED is significantly higher in the epicardial wall portion as compared to the endocardial wall portion (epicardial 8,087±116 dpm/mm^2 vs endocardial 6,378±524 dpm/mm^2, $p<0.05$; Fig. 2), which is consistent with the physiological distribution of sympathetic nerves in the healthy rat heart. On the other hand, there was no significant difference when comparing the accumulation of ^{131}I-MIBG between the epicardial and the endocardial wall portion (epicardial 7,926±98 dpm/mm^2 vs endocardial 7,594±262 dpm/mm^2, n.s.; Fig. 2).

Analyzing rat hearts 2 months after coronary occlusion and reperfusion revealed the following results (Fig. 3): the scar area showed an extent of 4.0±2.4 % as determined by VVG staining, and there was no significant difference to the uptake defect of ^{131}I-MIBG which was found to be 3.8±2.3 % (n.s.). Furthermore, there was a significant correlation between the scar area and the ^{131}I-MIBG defect which almost showed unity ($y=0.98x+0.3$, $R^2=0.94$, $p<0.01$). However, the defect size of HED clearly exceeded both the ^{131}I-MIBG defect and the scar area (9.1±2.2 %, $p<0.001$ vs scar/MIBG), reflecting the ischemic damage to sympathetic nerves which is known to be bigger than the infarction area [18].

Discussion

In the present study, we compared the uptake mechanism of the sympathetic nerve imaging tracers ^{11}C-HED and ^{123}I/^{131}I-MIBG in rat hearts after blockade of uptake-1 or both uptake-1 and -2 using the same experimental setting. HED uptake showed high specificity to neural uptake-1 in rat hearts indicating favorable characters for sympathetic nerve imaging. However, it is of note that MIBG uptake in the early phase after tracer injection demonstrated significant contribution of nonneural uptake-2 in rat hearts. In addition, we directly compared the regional distribution of these two tracers in a rat model of ischemia/reperfusion and in control hearts using a dual-tracer autoradiographic approach. We again found significant differences in the distribution pattern between HED and ^{123}I/^{131}I-MIBG.

We used desipramine and phenoxybenzamine to block either uptake-1 alone, or both uptake-1 and -2, in our ex vivo tissue counting experiment, respectively. Desipramine is one of the most potent uptake-1 inhibitors and has been evaluated in a large number of studies both in animals including rats hearts as well as in humans [19–22]. Also, phenoxybenzamine is well known as an uptake-1 and -2 inhibitor and was shown in a study of the isolated perfused

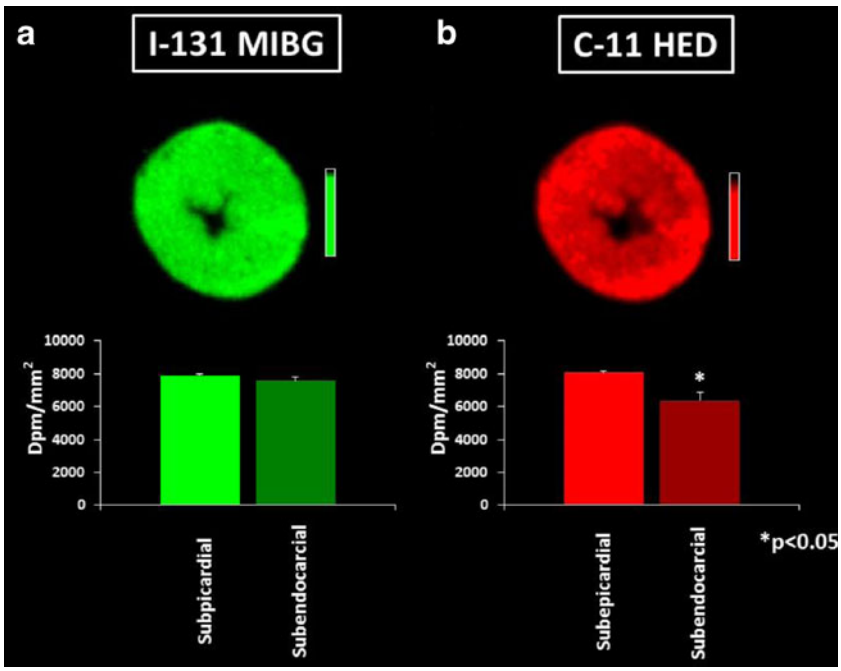

Fig. 2 Short axis slices of the dual-tracer autoradiography study using ^{131}I-MIBG and HED. ROIs were drawn in the subepicardial and in the subendocardial wall portion to compare tracer distribution. ^{131}I-MIBG demonstrates an even distribution throughout the myocardium (**a**), while HED shows a gradient from the subepicardial to the subendocardial wall portion (**b**)

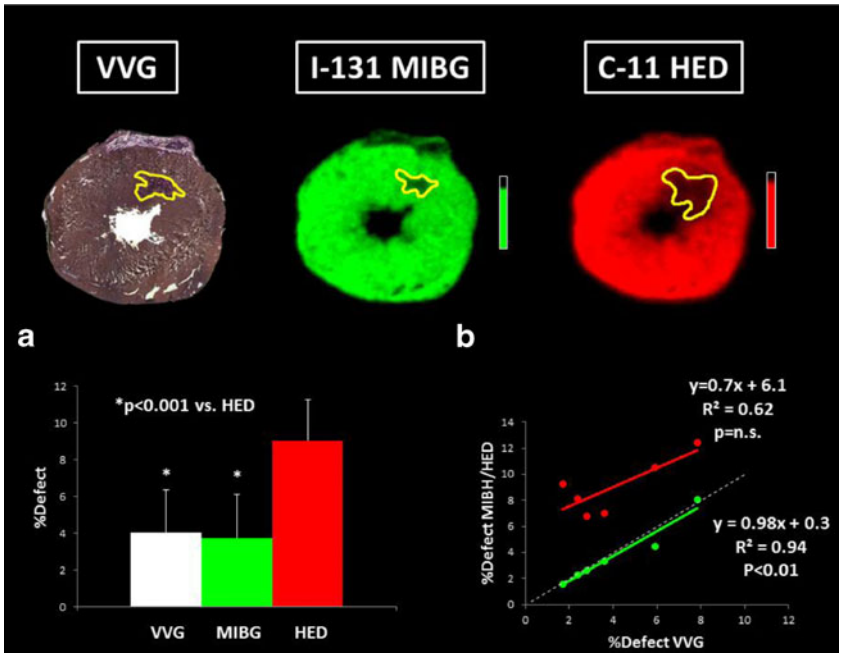

Fig. 3 Representative short axis slices of Verhoeff-van Gieson (VVG) staining, ^{131}I-MIBG, and HED distribution in a rat model of chronic ischemia/reperfusion. Scar area using VVG staining and uptake defect sizes using ^{131}I-MIBG or HED images were identified. Scar area and ^{131}I-MIBG defect area are significantly smaller than the HED defect (**a**). There is close correlation between the scar area and the ^{131}I-MIBG defect almost reaching unity (**b**, *broken white line* represents line of unity)

rat heart to be able to block both mentioned uptake mechanisms by about 88 % [20, 23].

MIBG tracers were kindly provided by GE Healthcare and showed both high specific activity and radiochemical purity. MIBG was used within 2 h after calibration time at the supplier. Regarding the relatively long half-life of ^{123}I or ^{131}I, respectively, this short delay should not significantly alter these specifications. HED was synthesized as previously described at our institution [13], also revealed both high specific activities and radiochemical purities, and was used directly after synthesis. High specific activities are an important prerequisite in this study, as with low specific activity the specific uptake should be less pronounced.

Our ex vivo tissue counting study showed that for HED both the uptake-1 blockade with desipramine and uptake-1 and -2 blockade with phenoxybenzamine led to approximately 90 % decline in the H/B ratio. These results indicate that HED is specifically taken up by the uptake-1 and only to a negligible amount by the uptake-2 in rat hearts. This is consistent with one of the early experiments using the isolated perfused rat heart where strong inhibitory effects of uptake-1 blockade with desipramine to the cardiac HED accumulation were demonstrated [22]. Another recent report showed that HED uptake to the heart, which was assessed by in vivo small animal PET imaging, could be effectively blocked by desipramine [19]. Moreover, we analyzed the local distribution pattern of HED uptake using an autoradiographic imaging assay. Interestingly, the HED image demonstrated a decreasing gradient from the subepicardium to the subendocardium in the healthy rat hearts. This transmural pattern of sympathetic nerve distribution is also reported in mice hearts and was assessed by tyrosine hydroxylase (TH) immunofluorescence staining [24]. Our preliminary evaluation with TH staining in the healthy rat heart found a similar gradient of innervation (1:0.29, ratio of nerve density between subepicardium and subendocardium). Therefore, the tracer distribution pattern could be a reflection of the physiological sympathetic innervation in rat hearts. Furthermore, in the coronary occlusion and reperfusion model, we found that the HED defect exceeded the scar area. Since we used a rat model of transient coronary occlusion and reperfusion (20 min), the scar area was observed to be only a small proportion within the area at risk [7]. In patients suffering from myocardial infarction, it is known that the damage to sympathetic nerves exceeds the infarct size and represents the area at risk [18]. Therefore, our observation of the HED defect exceeding the scar area may reflect the area of ischemic damage to sympathetic nerves during coronary occlusion.

In contrast to the HED blockade study, ^{123}I-MIBG uptake was not affected by the uptake-1 blockade with desipramine even though both experiments were conducted using exactly the same protocol. In addition, since the uptake was decreased by more than 80 % after administration of the uptake-1 and -2 blocker phenoxybenzamine, these results indicate that ^{123}I-MIBG is taken up to a certain degree by the nonneural uptake-2 into the rat heart and only to a limited degree by both the uptake-1 and the nonspecific extracellular uptake. Furthermore, in the autoradiographic study in healthy rat hearts, ^{131}I-MIBG was distributed evenly throughout the myocardium. This result may also indicate high uptake-2 contribution by cardiomyocytes, which are evenly distributed throughout the left ventricle, as the physiological pattern of sympathetic nerve distribution from the subepicardium to the subendocardium was not reflected by

this study. Finally, the defect in the uptake of ^{131}I-MIBG in the model of chronic ischemia/reperfusion closely correlated with the scar area which again showed a distinct pattern from the HED defect that clearly exceeded the scar area.

Our results suggest that there are species-dependent differences in uptake-1 and -2 components. Data on the direct comparison of the affinity of HED and MIBG to the uptake mechanisms in different species are rare. Several studies suggest that the affinity of both substances is comparable [25]. Another point that needs to be considered, however, is the density of the uptake mechanisms, which is known to differ in species [26]. Studies suggest that humans have the highest density of the uptake-1 when comparing to dogs, rats, and rabbits. Consequently, humans may have a higher contribution of uptake-1 to the removal of catecholamines from the synaptic cleft when compared to animals.

In a study by Sisson et al. similar results were obtained [27]. This group assessed the cardiac uptake of ^{125}I-MIBG and ^{3}H-norepinephrine (^{3}H-NE) in rat hearts. Interestingly, this group found that the uptake of ^{3}H-NE was significantly more reduced by uptake-1 blockade or even after the selective destruction of noradrenergic neurons by the application of 6-hydroxydopamine. Although, a direct comparison to our study may not be feasible as different rat species (female Sprague-Dawley rats) were used. Another study which points out the differences in catecholamine handling in different animals was conducted by Tobes et al. [28]. In this study pretreatment with desipramine even led to an increase of the cardiac ^{125}I-MIBG uptake in dogs, indicating that the dog might also not be an ideal model to study cardiac sympathetic innervation if conclusions about humans are thought to be drawn. In a recent publication, Yu and colleagues demonstrated in an ex vivo tissue counting study that pretreatment with desipramine 1 mg/kg in rabbits leads to a 53 % decrease of the ^{123}I-MIBG uptake to the heart at 1 h after tracer injection [29]. Accordingly, when using the catecholamine analogue tracer ^{123}I-MIBG, the rabbit might be a better animal model for sympathetic nerve imaging since the specificity for neural uptake-1 seems to be higher in rabbits than the specificity in rat hearts as indicated by our experiments. For this reason, the combination of animal model and tracer for the purpose of studying sympathetic nerve imaging needs to be chosen carefully.

The specificity of MIBG for neural uptake-1 in the human heart is well documented by ^{123}I-MIBG imaging early after heart transplantation showing absence of tracer accumulation in the heart [30]. During the transplantation process, the allograft becomes completely denervated and reinnervation occurs in the time course of 1 year post-transplantation. In addition, the prognostic value of MIBG imaging is reported in several clinical studies. For example, in the prospective ADMIRE-HF study (AdreView Myocardial Imaging for Risk Evaluation in Heart Failure), 961 patients with heart failure were studied [2]. In a subsequent multivariate analysis, it was demonstrated that patients with a low heart to mediastinum ratio and, thus, less uptake of ^{123}I-MIBG in the heart, were at higher risk for both cardiac and all-cause death independent of other factors like ejection fraction, age, or brain natriuretic peptide (BNP) [2]. Unlike those clinical reports, our experiment data in rat hearts showed high contribution of nonneural uptake-2 for MIBG uptake.

These facts indicate that tracers utilizable in humans might not be always appropriate for research purposes in certain animal models. The growing clinical use of and interest in cardiac sympathetic nerve imaging justifies even more detailed investigation of catecholamine handling both in animals and in humans. Our study should be seen as a stimulus for additional research of the available sympathetic nerve imaging tracers to help elucidate the underlying complex uptake mechanisms.

Conclusion

Even though HED and ^{123}I-MIBG are established norepinephrine analogue tracers for use in clinical practice in human hearts, animal models must be chosen carefully using these tracers. Our results indicate that the accumulation of ^{123}I-MIBG in the rat heart has a high contribution of nonneural uptake-2, while HED is mainly and specifically taken up by neural uptake-1 into sympathetic nerve terminals. HED is suitable for sympathetic nerve imaging when conducting rat experiments, while ^{123}I-MIBG shows distinct species variations in the uptake contributions of uptake-1 and -2 when compared to the human heart.

Acknowledgments We thank Jennifer Merrill, Paige Finley, Jim Engles, James Fox and Gilbert Green for their excellent research assistance, and for the appreciated work of Daniel P. Holt and the whole cyclotron team. Also, we would like to thank Gola Javadi for her careful editorial assistance. This project was supported in part by an Investigator Initiated Grant (IIG) from GE Healthcare to TH and FB and by the National Institutes of Health grant 1RO1HL092985.

References

1. Hartikainen J, Mustonen J, Kuikka J, Vanninen E, Kettunen R. Cardiac sympathetic denervation in patients with coronary artery disease without previous myocardial infarction. Am J Cardiol 1997;80:273–7.
2. Jacobson AF, Senior R, Cerqueira MD, Wong ND, Thomas GS, Lopez VA, et al. Myocardial iodine-123 meta-iodobenzylguanidine imaging and cardiac events in heart failure. Results of the prospective ADMIRE-HF (AdreView Myocardial Imaging for Risk Evaluation in Heart Failure) study. J Am Coll Cardiol 2010;55:2212–21. doi:10.1016/j.jacc.2010.01.014.
3. Watson AM, Hood SG, May CN. Mechanisms of sympathetic activation in heart failure. Clin Exp Pharmacol Physiol 2006;33:1269–74. doi:10.1111/j.1440-1681.2006.04523.x.

4. Verberne HJ, Brewster LM, Somsen GA, van Eck-Smit BL. Prognostic value of myocardial 123I-metaiodobenzylguanidine (MIBG) parameters in patients with heart failure: a systematic review. Eur Heart J 2008;29:1147–59.
5. Pietilä M, Malminiemi K, Ukkonen H, Saraste M, Någren K, Lehikoinen P, et al. Reduced myocardial carbon-11 hydroxyephedrine retention is associated with poor prognosis in chronic heart failure. Eur J Nucl Med 2001;28:373–6.
6. Hartmann F, Ziegler S, Nekolla S, Hadamitzky M, Seyfarth M, Richardt G, et al. Regional patterns of myocardial sympathetic denervation in dilated cardiomyopathy: an analysis using carbon-11 hydroxyephedrine and positron emission tomography. Heart 1999;81:262–70.
7. Higuchi T, Bengel FM, Seidl S, Watzlowik P, Kessler H, Hegenloh R, et al. Assessment of alphavbeta3 integrin expression after myocardial infarction by positron emission tomography. Cardiovasc Res 2008;78:395–403.
8. Higuchi T, Fukushima K, Xia J, Mathews WB, Lautamäki R, Bravo PE, et al. Radionuclide imaging of angiotensin II type 1 receptor upregulation after myocardial ischemia-reperfusion injury. J Nucl Med 2010;51:1956–61. doi:10.2967/jnumed.110.079855.
9. Higuchi T, Anton M, Saraste A, Dumler K, Pelisek J, Nekolla SG, et al. Reporter gene PET for monitoring survival of transplanted endothelial progenitor cells in the rat heart after pretreatment with VEGF and atorvastatin. J Nucl Med 2009;50:1881–6.
10. Higuchi T, Bengel FM. Cardiovascular nuclear imaging: from perfusion to molecular function: non-invasive imaging. Heart 2008;94:809–16.
11. Higuchi T, Nekolla SG, Jankaukas A, Weber AW, Huisman MC, Reder S, et al. Characterization of normal and infarcted rat myocardium using a combination of small-animal PET and clinical MRI. J Nucl Med 2007;48:288–94.
12. Gallagher AM, Bahnson TD, Yu H, Kim NN, Printz MP. Species variability in angiotensin receptor expression by cultured cardiac fibroblasts and the infarcted heart. Am J Physiol 1998;274: H801–9.
13. Rosenspire KC, Haka MS, Van Dort ME, Jewett DM, Gildersleeve DL, Schwaiger M, et al. Synthesis and preliminary evaluation of carbon-11-meta-hydroxyephedrine: a false transmitter agent for heart neuronal imaging. J Nucl Med 1990;31:1328–34.
14. Guide for the care and use of laboratory animals. 8th edition Washington, DC: National Academies Press (US); 2011.
15. Higuchi T, Taki J, Nakajima K, Kinuya S, Namura M, Tonami N. Time course of discordant BMIPP and thallium uptake after ischemia and reperfusion in a rat model. J Nucl Med 2005;46:172–5.
16. Taki J, Higuchi T, Kawashima A, Tait JF, Kinuya S, Muramori A, et al. Detection of cardiomyocyte death in a rat model of ischemia and reperfusion using 99mTc-labeled annexin V. J Nucl Med 2004;45:1536–41.
17. Schneider CA, Rasband WS, Eliceiri KW. NIH Image to ImageJ: 25 years of image analysis. Nat Methods 2012;9:671–5.
18. Matsunari I, Schricke U, Bengel FM, Haase HU, Barthel P, Schmidt G, et al. Extent of cardiac sympathetic neuronal damage is determined by the area of ischemia in patients with acute coronary syndromes. Circulation 2000;101:2579–85.
19. Tipre DN, Fox JJ, Holt DP, Green G, Yu J, Pomper M, et al. In vivo PET imaging of cardiac presynaptic sympathoneuronal mechanisms in the rat. J Nucl Med 2008;49:1189–95.
20. Iversen LL. Catecholamine uptake processes. Br Med Bull 1973;29:130–5.
21. Malizia AL, Melichar JK, Rhodes CG, Haida A, Reynolds AH, Jones T, et al. Desipramine binding to noradrenaline reuptake sites in cardiac sympathetic neurons in man in vivo. Eur J Pharmacol 2000;391:263–7.
22. DeGrado TR, Hutchins GD, Toorongian SA, Wieland DM, Schwaiger M. Myocardial kinetics of carbon-11-meta-hydroxyephedrine: retention mechanisms and effects of norepinephrine. J Nucl Med 1993;34:1287–93.
23. Iversen LL, Salt PJ, Wilson HA. Inhibition of catecholamine uptake in the isolated rat heart by haloalkylamines related to phenoxybenzamine. Br J Pharmacol 1972;46:647–57.
24. Ieda M, Kanazawa H, Kimura K, Hattori F, Ieda Y, Taniguchi M, et al. Sema3a maintains normal heart rhythm through sympathetic innervation patterning. Nat Med 2007;13:604–12.
25. Raffel DM, Chen W, Jung YW, Jang KS, Gu G, Cozzi NV. Radiotracers for cardiac sympathetic innervation: transport kinetics and binding affinities for the human norepinephrine transporter. Nucl Med Biol 2013;40:331–37.
26. Raffel DM, Chen W. Binding of [3H]mazindol to cardiac norepinephrine transporters: kinetic and equilibrium studies. Naunyn Schmiedebergs Arch Pharmacol 2004;370:9–16.
27. Sisson JC, Wieland DM, Sherman P, Mangner TJ, Tobes MC, Jacques Jr S. Metaiodobenzylguanidine as an index of the adrenergic nervous system integrity and function. J Nucl Med 1987;28:1620–4.
28. Tobes MC, Jaques Jr S, Wieland DM, Sisson JC. Effect of uptake-one inhibitors on the uptake of norepinephrine and metaiodobenzylguanidine. J Nucl Med 1985;26:897–907.
29. Yu M, Bozek J, Lamoy M, Guaraldi M, Silva P, Kagan M, et al. Evaluation of LMI1195, a novel 18F-labeled cardiac neuronal PET imaging agent, in cells and animal models. Circ Cardiovasc Imaging 2011;4:435–43.
30. Estorch M, Campreciós M, Flotats A, Marí C, Bernà L, Catafau AM, et al. Sympathetic reinnervation of cardiac allografts evaluated by 123I-MIBG imaging. J Nucl Med 1999;40:911–6.